Heterogeneous Combustion of Aluminized Propellants

R.P. Rastogi,* K. Kishore,† and Desh Deepak‡
University of Gorakhpur, Gorakhpur, India

Hybrid combustion of an aluminized polystyrene/oxygen system has been investigated. The mass consumption rate of the fuel is found to be proportional to the square root of the mass consumption rate of the oxidizer. The regression rate depends on time, as was found to be the case for an unmetallized propellant. The role of radiative heat transfer to the combustion products and unreacted oxidizer is confirmed when the data are analyzed in the context of the theory of Marxman et al. Analysis of the data takes into account the heat taken away by metal particles during combustion. This is found to be strongly dependent on the oxidizer flow rate.

Nomenclature

a, a'	= constants that are functions of time
A	= initial duct radius, cm
A_p	= effective port area
B	= thermochemical mass-transfer number
C	= mean particle concentration, mg/liter
C_m	= heat capacity of nonvaporizing fuel component
D	= instantaneous duct diameter, cm
g	= mass of the particulates in the duct at any time
G	= total mass flux, g/cm^2-sec
G_{ox}	= initial oxidizer mass flux, g/cm^2-sec
h_{vb}	= heat of gasification of binder material
$h_{v_{eff}}$	= effective heat of gasification of solid phase
K	= mass fraction of nonvolatile surface material
K_m	= absorption term averaged with respect to the thermal spectrum, liter/mg-cm
l	= length of the grain, cm
L	= mean beam path length, cm
$\dot{m}_f$	= mass flow rate of the fuel, g/sec
$\dot{m}_g$	= total gas flow rate, g/sec
$\dot{m}_{ox}$	= mass flow rate of the oxidizer, g/sec
n, n'	= constants that are function of time
N	= constant $2g\, K_m/\pi \ell$
p^*	= dimensionless pressure
P	= internal perimeter of fuel grain
P_r	= Prandtl number
$\dot{Q}_c$	= conductive heat transfer to the fuel surface in the absence of radiation
$\dot{Q}_p$	= heat taken away by the particulate combustion products
$\dot{Q}_r$	= radiative heat transfer to the fuel surface
$\dot{Q}_{re}$	= net heat transfer from the flame zone to the combustion products and unreacted oxidizer by radiation
$\dot{Q}_T$	= total heat produced in the flame zone
$\dot{Q}_W$	= net heat transported to the fuel surface from the flame zone
r	= instantaneous radius of the duct, cm
$\dot{r}$	= regression rate, cm/sec
t	= time, sec
ΔT	= temperature difference between the surface and an ambient point deep in the grain
T_c	= equilibrium temperature of the internal core of combustion products and unreacted oxidizer
T_i	= temperature of the flame zone
T_r	= effective radiation temperature
x	= longitudinal coordinate
y	= constant
z	= constant
α_i	= absorption of the flame zone at temperature T_c
β	= empirical pressure exponent
δ	= boundary-layer displacement thickness
ϵ_c	= emissivity of combustion products in the internal core
ϵ_g	= emissivity of radiating continuum
ϵ_i	= emissivity of the flame zone at temperature T_i
ϵ_w	= wall absorptivity
θ	= mass of oxidizer consumed in producing particulate combustion products per unit mass of the nonvolatile surface material that forms particulate products
μ	= viscosity
$\bar{\rho}$	= reference density
ρ_e	= density at the edge of boundary layer or on motor centerline
ρ_f	= density of fuel
ρ_v	= bulk density of volatile component of the fuel
σ	= Stefan-Boltzmann constant
τ	= weight fraction of gas in decomposed fuel grain at equilibrium wall temperature

Subscripts

f	= fuel
0	= zero time
ox	= oxidizer
t	= any time

Received January 20, 1975; revision received June 3, 1975. D. Deepak is thankful to the Council of Scientific and Industrial Research, India, for financial support.

Index categories: Fuels and Propellants, Properties of; Combustion in Heterogeneous Media; Solid and Hybrid Rocket Engines.

*Senior Professor of Chemistry, Department of Chemistry. Associate Fellow AIAA.

†Presently Assistant Professor, Department of Inorganic and Physical Chemistry, Indian Institute of Sciences, Bangalore, India.

‡Senior Research Fellow, Department of Chemistry.

I. Introduction

METALLIZED propellant systems for hybrid rockets are of interest because metal additives increase the flame temperature and its emissivity.[1] It has been pointed out that coupling between convective and radiative heat transfer can give rise to new ways of controlling regression rate mechanism.[2] Radiation effects have been considered by Fineman[3] and Marxman et al.[4] Smoot and Price[5-7] have investigated experimentally the pressure dependence of regression rate for the case of metallized and unmetallized propellants. They ascribed it to the participation of heterogeneous surface reactions as the rate-limiting process. Very recently, Rastogi et al.[8,9] have investigated hybrid combustion characteristics using boron containing polyesters/oxygen and polystyrene and styrene copolymer/oxygen systems. Decrease of instantaneous regression rate with time is observed, and the results have been analyzed in terms of an analytical theory, which takes into account the radiative heat transfer from the flame zone to the combustion products and unreacted oxidizer. It was thought to perform a corresponding study of hybrid combustion of an aluminized propellant system in view of its practical utility and in view of intrinsic theoretical interest in the combustion process, where additional sources and sinks of radiation are present. Regression rate measurements have been made for aluminized propellants of different composition at different flow rates. The results have been correlated using a mathematical theory, and useful conclusions have been drawn.

II. Theory

The most comprehensive investigation of heat-transfer-limited combustion in reacting turbulent boundary layers is due to Marxman et al.[4,10] and is based on the preliminary hybrid combustion study of Marxman and Gilbert.[11] The hybrid regression rate is given by[12]

$$\rho_v \dot{r} = \rho_f (1-K) \dot{r} = (\dot{Q}_c / h_{v_{\rm eff}}) \, [(\dot{Q}_r/\dot{Q}_c) + \exp^{-\dot{Q}_r/\dot{Q}_c}] \tag{1}$$

where

$$\dot{Q}_c = 0.036 (\bar{\rho}/\rho_e)^{0.6} h_{v_{\rm eff}} p^{*0.23\beta} B^{0.23} (x/\mu)^{-0.2} (\dot{m}_g / A_p)^{0.8} \tag{2}$$

$$\dot{Q}_r = \sigma \epsilon_w \epsilon_g p^{*\beta} T_r^4 \tag{3}$$

It is important to note that $\dot{Q}_c$ is the convective heat transfer under the given flow condition in the absence of radiation.[10] The empirical dimensionless pressure term $p^{*\beta}$ has been incorporated to account for the observed pressure effects. The bulk density of the volatile component of fuel is the density that determines the magnitude of $\dot{r}$, because the volumetric flow rate of particles from the surface is negligible compared to the volumetric flow of the gas.[12] The effective heat of gasification is represented by

$$h_{v_{\rm eff}} = h_{vb} + [K/(1-K)] \cdot C_m \Delta T \tag{4}$$

$h_{v_{\rm eff}}$ is the sum of the heat necessary to gasify the volatile components of the fuel plus the heat necessary to heat the nonvolatile component to the surface temperature.

Applying the simple heat balance equation for the combustion of metallized propellant, in a thin flame zone of the turbulent boundary layer over the vaporizing surface, entirely governed by the mixing dynamics, we have

net heat transported to the fuel surface from the flame zone
= [heat transfer by convection and radiation]
= [total heat produced in the flame zone]
− [net heat transfer from the flame
to the combustion products and unreacted oxidizer
by radiation
+ heat taken away by the particulate
combustion products]

Hence, with the help of Eq. (1), we can write

$$\dot{Q}_w = \rho_f (1-K) \dot{r} \, h_{v_{\rm eff}} = \dot{Q}_T - [\dot{Q}_{\rm re} + \dot{Q}_p] \tag{5}$$

Now at a particular time,

$$\dot{r}_t = \frac{\dot{Q}_T}{\rho_f (1-K) h_{v_{\rm eff}}} - \frac{\dot{Q}_{re} + \dot{Q}_p}{\rho_f (1-K) h_{v_{\rm eff}}} \tag{6}$$

When $t=0$,

$$[(\dot{Q}_{\rm re} + \dot{Q}_p)/\rho_f (1-K) h_{v_{\rm eff}}] = 0$$

and at that instant

$$\dot{r}_t = \dot{r}_0 = \dot{Q}_T / [\rho_f (1-K) h_{v_{\rm eff}}] \tag{7}$$

Combining Eqs. (6) and (7), we get

$$\dot{r}_t = \dot{r}_0 - \frac{\dot{Q}_{\rm re}}{\rho_f (1-K) h_{v_{\rm eff}}} - \frac{\dot{Q}_p}{\rho_f (1-K) h_{v_{\rm eff}}} \tag{8}$$

Since radiative heat transfer from the flame zone to the combustion products and unreacted oxidizer would increase due to increase in the proportion of unburnt oxidizer and combustion products with the increase in the duct diameter, the factor $\dot{Q}_{\rm re}/\rho_f (1-K) h_{v_{\rm eff}}$ would increase, and thus instantaneous regression rate would decrease with time.

The radiative heat transfer from the flame zone to the combustion product and unreacted oxidizer would be given by the following equation:

$$\dot{Q}_{\rm re} = \sigma T_i^4 \epsilon_i - \sigma T_c^4 \epsilon_c \alpha_i \tag{9}$$

Substituting Eq. (9) in Eq. (8) and rearranging, we have

$$\dot{r}_t = \dot{r}_0 + \frac{\sigma T_c^4 \epsilon_c \alpha_i}{\rho_f (1-K) h_{v_{\rm eff}}} - \frac{\dot{Q}_p + \sigma T_i^4 \epsilon_i}{\rho_f (1-K) h_{v_{\rm eff}}} \tag{10}$$

In the present case, gas radiation can be neglected because the radiation of the particulates is much more significant than the gas radiation.[12] Burning metal particles and their oxides behave as the particle clouds in the flame and act as radiation centers. It is to be noted that the emissivity of the flame is constant in this case. The emissivity of particle clouds in the internal gas core of combustion products and unreacted oxidizer in the tubular grain can be represented as follows[13,14]:

$$\epsilon_c = 1 - \exp(-CL\,K_m) \tag{11}$$

The mean beam path length L may be taken equivalent to the radius of gas hemisphere, which gives out the same amount of radiation as the actual gas mass, to unit area at the center of its base. In case of hybrid combustion in a tubular grain, while considering the emissivity of the internal gas core of combustion products and unreacted oxidizer, L may be taken as the duct diameter.

Equation (11) can be transformed in the following form:

$$\epsilon_\phi = 1 - \exp[-(g/\pi r^2 l) 2r \cdot K_m) = 1 - \exp[-N/r] \tag{12}$$

where $C = g/\pi r^2 l, L = 2r$, and $N = 2gK_m/\pi l$

The emissivity of burning Al particles and of heated Al_2O_3 is reported[1] to be of the order of 0.1. It indicates that the magnitude of N/r is less than 1. Accordingly, expanding exp $(-N/r)$ in Eq. (12) and neglecting the higher powers, we get

$$\epsilon_c \simeq N/r \tag{13}$$

It is obvious that the function N is constant for a particular fuel composition and oxidizer flow rate. The temperature T_c is the equilibrium temperature of the internal core and can be assumed to be constant as a first approximation. Therefore, from Eqs. (10) and (13), we have

$$(\dot{r}_0 - \dot{r}_t) = \left[\frac{\dot{Q}_p + \sigma T_i^4 \epsilon_i}{\rho_f (1-K) h_{v_{\rm eff}}} \right] - \left[\frac{\sigma T_c^4 \alpha_i N}{\rho_f (1-K) h_{v_{\rm eff}}} \right] \frac{1}{r} \tag{14}$$

The factor $[\dot{Q}_p + \sigma T_i^4 \epsilon_i]/\rho_f(1-K)h_{e_{\rm eff}}$ in Eq. (14) remains constant for a particular fuel composition and oxidizer flow rate. Equation (14) can be used to examine the contribution of radiative heat transfer from the flame zone to the internal core of combustion products and unreacted oxidizer in case of metallized hydrid rocket propellants.

III. Experimental

A. Preparation of Aluminized Polymer Sample

Styrene monomer was polymerized using benzoyl peroxide. In the viscous polymer, the aluminium powder of definite particle size was mixed mechanically. A homogeneous polymer was obtained. The density of the samples was found to be constant.

B. Regression Rate Studies

The hybrid burner was similar to that described earlier.[9] The experiments were performed for aluminized propellants at different oxygen flow rates and metal loadings. The duct radius was measured at various time intervals for each flow rate of the oxidizer. Data fitted the following equation:

$$r = A + z \cdot t^y \tag{15}$$

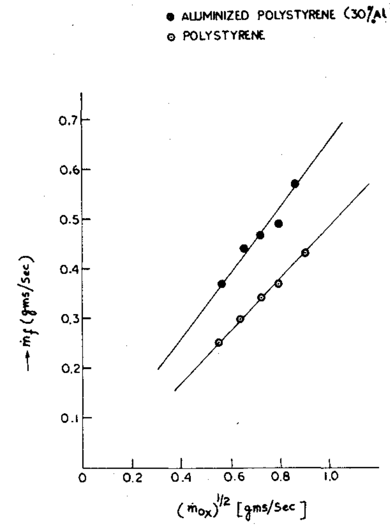

Fig. 1 Plot of mass flow rate of the fuel vs square root of the oxidizer flow rate. (The lines are best fit, and the points are data.)

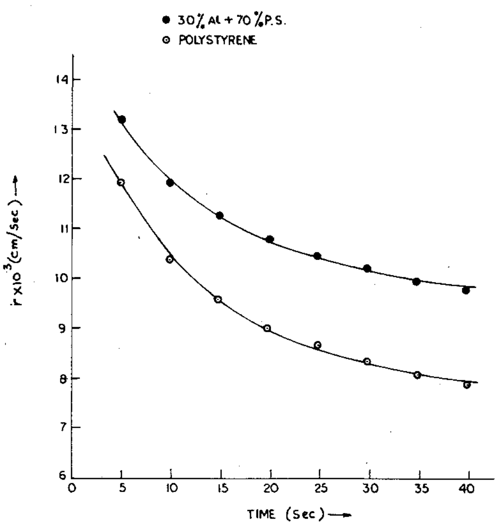

Fig. 2 Plot of regression rate vs time. (The lines are best fit, and the points are data.)

where y and z are constants. These were determined from the experimental data by plotting $\log(r - A)$ against $\log t$. Regression rate was obtained by differentiating Eq. (15). The particle size of aluminum also was varied. The mass flow rate of fuel $\dot{m}_f$ was evaluated in each case by measuring weight loss of the sample at different burn times. All the measurements were made at atmospheric pressure.

C. Flame Temperature Measurements

The flame temperature was measured by using sodium line reversal technique.[15] The iodine-filled tungsten filament lamp was used as a standard source. The procedure was similar to that described earlier.[9]

IV Analysis of Results

Experimental results showed that mass flow rate of the fuel $\dot{m}_f$ remains constant throughout the burning time for a particular flow rate of the oxidizer and different metal loadings. Figure 1 shows that mass flow rate of the fuel is related to mass flow rate of the oxidizer in the following manner:

$$\dot{m}_f = \text{const } \dot{m}_{\rm ox}^{0.5} \tag{16}$$

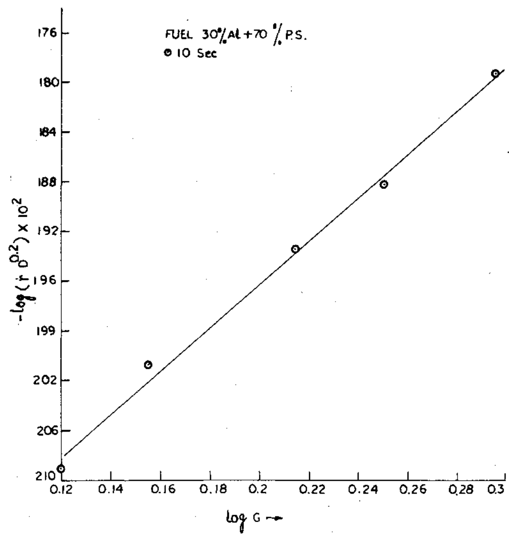

Fig. 3 Least-squares plot of $-\log(\dot{r}D^{0.2})$ vs log G at shorter burning time.

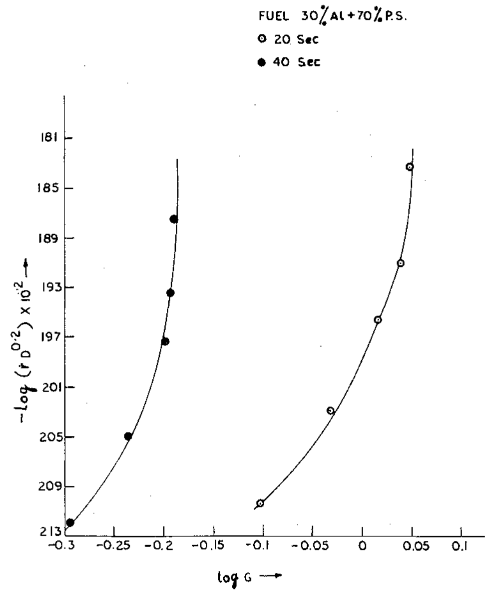

Fig. 4 Plot of $-\log(\dot{r}D^{0.2})$ vs log$G$ at higher burning times. (The lines are best fit, and the points are data.)

Because of this, O/F ratio remains constant throughout the burning. In Fig. 1, $\dot{m}_f$ values of this aluminized propellant system at various oxidizer flow rates have been compared with those for an unmetallized propellant system. It is found that $\dot{m}_f$ values for aluminized polystyrene are higher than those for the unmetallized one.

The comparison of $\dot{r}$ values for aluminized polystyrene with those for an unmetallized one, in Fig. 2, shows that regression rate increases when metal is added. Furthermore, it is observed that the regression rate decreases with time. It should be noted that increase in regression rate for the metallized propellant is greater at higher times compared to that at shorter burning times. This may be due to greater predominance of radiative heat transfer to the fuel surface, with increasing time.

Smoot and Price[5,6] obtained the following regression rate equation for fully developed turbulent flow in cylindrical duct, taking into account the effect of condensed species at the wall

$$\dot{r}=0.023(G^{0.8}/\tau\rho_f)(\mu/D)^{0.2}\ln[1+(B\tau/P_r^{2/3})] \quad (17)$$

which can be represented as

$$\dot{r}D^{0.2}=aG^n \quad (18)$$

where

$$a=(0.023/\rho_f\tau)(\mu)^{0.2}\ln[1+(B\tau/P_r^{2/3})]$$

and where $n=0.8$.

To test Eq. (18), $\log(\dot{r}D^{0.2})$ was plotted against $\log G$ in Figs. 3 and 4. Equation (18) is obeyed for shorter burning times (Fig. 3). However, for longer burning times, deviations from Eq. (18) have been observed which become more marked as time increases (Fig. 4). It is probably because the radiative heat transfer becomes more prominant as duct diameter increases. It should be noted that Eq. (17) does not take into account the radiative-convective coupling.

For the calculation of total mass flux G, it is necessary to know total gas flow rate and effective port area. The total gas flow rate $\dot{m}_g$ was calculated using the following relation[12]

$$\dot{m}_g=\dot{m}_{ox}+\left(1-\frac{K\theta}{1-K}\right)\int_0^x \rho_v \dot{r}P\mathrm{d}x \quad (19)$$

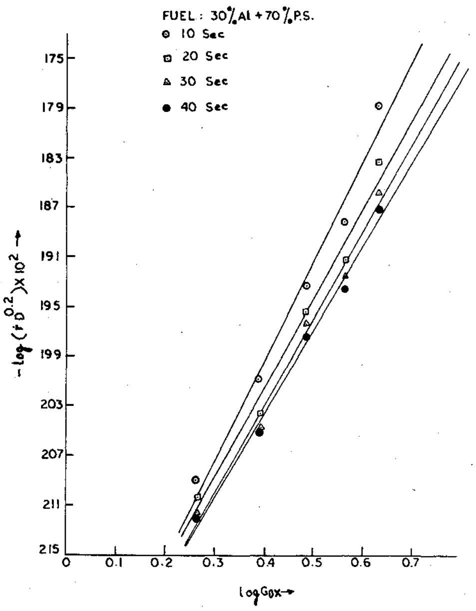

Fig. 5 Least-squares plot of $-\log(\dot{r}D^{0.2})$ vs $\log G_{ox}$.

θ was estimated by taking into account the following net reaction of aluminum combustion:

$$2Al+1.5\ O_2 \rightarrow Al_2O_3$$

The following relation was used to calculate the effective port area A_p

$$A_p=(\pi/4)\ (D-2\delta)^2 \quad (20)$$

where $2\delta=0.21D$. In the present case, the hydraulic diameter D is equal to the diameter of the duct for a cylindrical grain.

In Fig. 5, $\log(\dot{r}D^{0.2})$ has been plotted against $\log G_{ox}$ in order to examine the relationship between $\dot{r}$ and initial oxidizer mass flux. Results show that the following equation is valid:

$$\dot{r}D^{0.2}=a'G_{ox}^{n'} \quad (21)$$

Both a' and n' are time-dependent, but variation in a' with time is very small, as is clear from Fig. 6.

To study the role of particle size of aluminum on regression rate, the regression rate measurements were made for propellants containing aluminum particles of size 150-75 and 75-53μ. The results are plotted in Fig. 7. The regression rates were found to be similar within experimental error. The role of aluminum particles in combustion appears to be as follows. First, since the melting point of aluminum is only 932°K and the flame temperature for 30% aluminized polystyrene at 2-

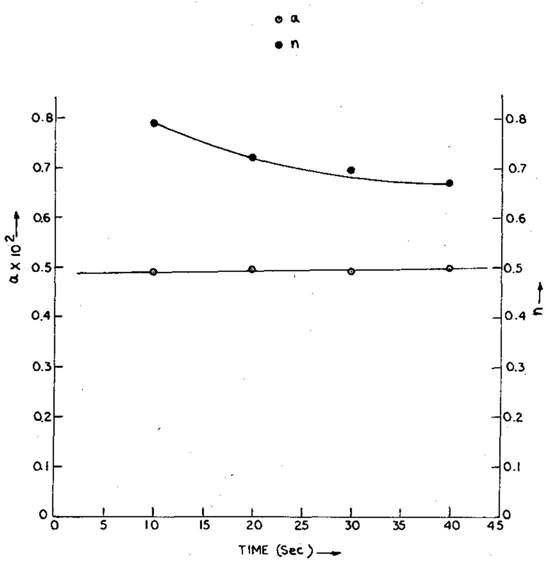

Fig. 6 Plot of a' and n' vs time. (The lines are best fit, and the points are data.)

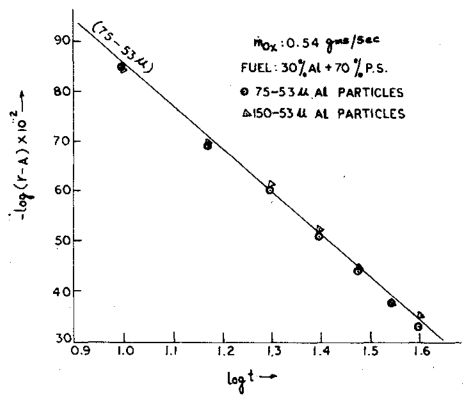

Fig. 7 Least-squares plot of $-\log(r-A)$ vs $\log t$; particle size of aluminum (75-53μ).

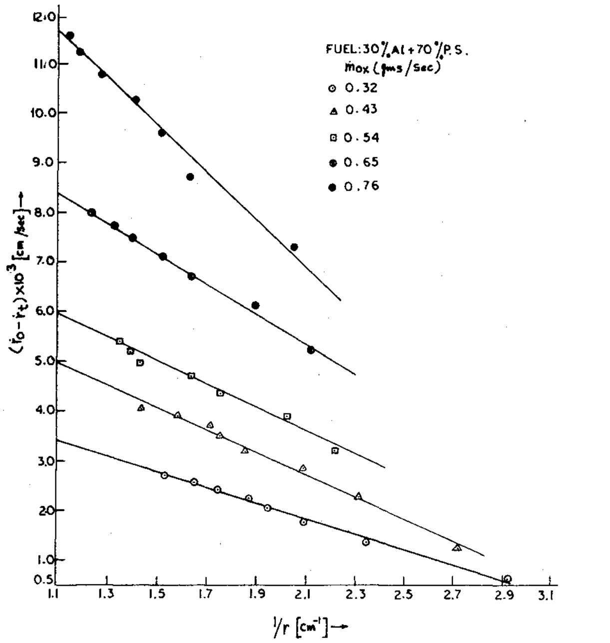

Fig. 8 Least-squares plot of $(\dot{r}_0 - \dot{r}_t)$ vs $1/r$ at various oxidizer mass flow rates.

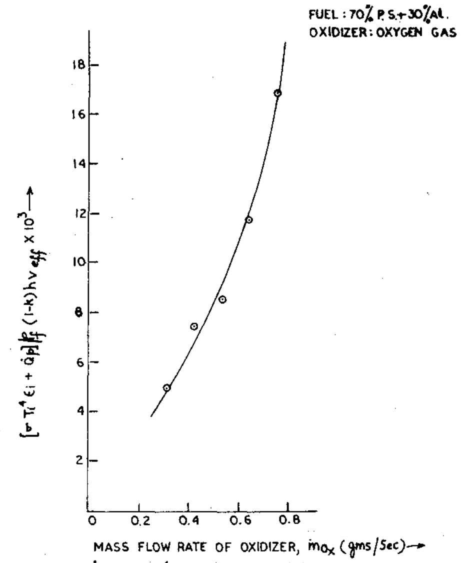

Fig. 9 Plot of $[\dot{Q}_p + \sigma T_i^4 \epsilon_i]/\rho_f(1-K)h_{v_{\rm eff}}$ vs oxidizer mass flow rate. (The lines are best fit, and the points are data.)

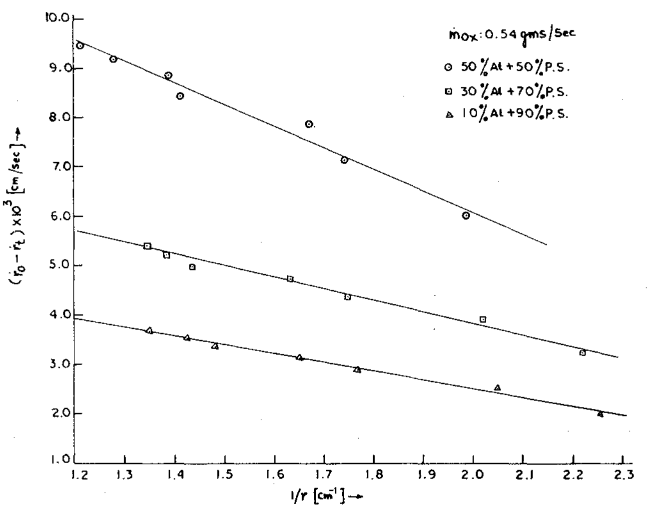

Fig. 10 Least-squares plot of $(\dot{r}_0 - \dot{r}_t)$ vs $1/r$ at various percentages of metal content in the fuel grain.

Table 1 Values of $[\dot{Q}_p + \sigma T_i^4 \epsilon_i]/\rho_f h_{v_{\rm eff}}$ at different aluminum compositions in the fuel ($\dot{m}_{ox} = 0.54$ g/sec)

Fuel composition	$[\dot{Q}_p + \sigma T_i^4 \epsilon_i]/\rho_f h_{v_{\rm eff}} \times 10^3$
10% Al + 90% polys'yrene	5.44
30% Al + 70% polystyrene	5.93
50% Al + 50% polystyrene	7.34

liter/min oxygen gas flow is 1833° ± 50°, it melts and forms a layer of aluminium oxide. Secondly, the particles also can be carried in the flame, where the size need not be the same as the original one. Hence, in effect, particle size becomes immaterial for controlling the regression rate within the range studied.

It has been suggested by Rastogi et al.[8,9] that decrease in regression rate with time is due to radiative heat transfer from the flame to the combustion products and unreacted oxidizer flowing through the duct. In order to test this view for metallized propellants, Eq. (14) was tested. Values of $(\dot{r}_0 - \dot{r}_t)$ were plotted against $1/r$ in Fig. 8 for various flow rates of the oxidizer. $\dot{r}_0$ was evaluated by extrapolating to zero time. Plots of the data in Fig. 8 clearly indicate that Eq. (14) is well satisfied at all the flow rates investigated, since straight lines are obtained. This confirms the important role of radiative heat transfer to the internal core of combustion products and unreacted oxidizer, in the combustion process. It should be noted that the slope of the straight lines in Fig. 8 is negative. This is in agreement with Eq. (14). Furthermore, the slope increases with increasing oxidizer flow rate. This is expected, since at higher flow rate both T_i and T_c would be higher. The factor $[\dot{Q}_p + \sigma T_i^4 \epsilon_i]/\rho_f(1-K)h_{v_{\rm eff}}$ was calculated for each flow rate from the intercept. The factor is plotted against oxidizer flow rate in Fig. 9. It increases rapidly with the increase in oxidizer flow rate. This also is expected, since the flame temperature would be higher, the greater the flow rate.

Equation (14) also was tested for the propellants with different aluminium percentage. Plots are shown in Fig. 10 which confirm the validity of Eq. (14) for the system, since straight lines are obtained and the slopes are negative. In this case also, both the slope and the intercept increase with increase in metal loading. This is in agreement with Eq. (14), since the slope would depend on N. Furthermore, T_i and T_c would increase with increase in N. The value of $[\dot{Q}_p + \sigma T_i^4 \epsilon_i]/\rho_f(1-K)h_{v_{\rm eff}}$ was evaluated from the intercept for different aluminized propellant combinations. A comparison of the values of $[\dot{Q}_p + \sigma T_i^4 \epsilon_i]/\rho_f h_{v_{\rm eff}}$ in Table 1 show unusually high values for 50% aluminized propellant, although the values for 10% and 30% aluminized fuel are similar within experimental error. It may be due to either increase in flame temperature with increased metal loading or different type of burning characteristic in the case of highly metal-loaded hybrid propellant. Since the thermal conductivity of aluminium is very high compared to that of polystyrene, the surface temperature of the burning fuel would be lowered because of conduction into the grain. High metal content, together with lowering of surface temperature, results in thickening of the protective aluminium oxide layer, which in turn effectively reduces the available fuel surface, and thus unusual reduction of the regression rate is observed at higher burning times. It was observed during investigation that the burning of 50% aluminized polystyrene propellant system is not smooth at higher time because of deposition of thick metal oxide layer at the fuel surface.

V. Conclusions

The following conclusions can be drawn from the present study:

1) The mass flow rate of the fuel varies linearly as the square root of the oxidizer mass flow rate.

2) Addition of aluminium in the polymer fuel increases the mass consumption rate of the fuel and the regression rate.

3) The equation $\dot{r} D^{0.2} = aG^n$ is valid at shorter burning times, but deviations become marked as time increases. This is because of increasing predominance of radiative heat transfer with increase in time. Furthermore, the regression rate is related to initial oxidizer mass flux, where a' and n' are time-dependent.

4) The regression rate decreases with time for a fixed flow rate of the oxidizer and for a particular propellant composition, because of radiative heat transfer from the flame zone to the combustion products and unreacted oxidizer flowing through the duct. The data satisfy Eq. (14), viz.,

$$(\dot{r}_0 - \dot{r}_t) = \left[\frac{\dot{Q}_p + \sigma T_i^4 \epsilon_i}{\rho_f (1-K) h_{v_{\text{eff}}}} \right] - \left[\frac{\sigma T_c^4 \alpha_i N}{\rho_f (1-K) h_{v_{\text{eff}}}} \right] \frac{1}{r}$$

5) Regression rate appears to be independent of particle size.

6) In the combustion of metallized hybrid propellant, the heat taken away by the particulate combustion products is an important factor to be taken into account. It is found that $[\dot{Q}_p + \sigma T_i^4 \epsilon_i] / \rho_f (1-K)\ h_{v_{\text{eff}}}$ increases very rapidly with oxidizer flow rate.

References

[1]Zennin, A.A., Glaskova, A.P., Leipunskyi, O.I., and Bobolev, V.K., "Effects of Metallic Additives on the Deflagration of Condensed Systems," *Proceedings of the Twelfth Symposium (International) on Combustion,* The Combustion Institute, Pittsburgh, Pa., 1969, pp. 27-35.

[2]Marxman, G.A., "Boundary Layer Combustion in Propulsion," *Proceedings of the Eleventh Symposium (International) on Combustion,* The Combustion Institute, Pittsburgh, Pa., 1967, pp. 269-289.

[3]Fineman, S., "Some Analytical Considerations of the Hybrid Rocket Combustion Problem," Master's thesis, 1962, Princeton University, Princeton, N.J.

[4]Marxman, G.A., Wooldridge, C.E., and Muzzy, R.J., "Fundamentals of Hybrid Boundary Layer Combustion," *AIAA Progress in Astronautics and Aeronautics: Heterogeneous Combustion,* Vol. 15, edited by H.G. Wolfhard, I. Glassman, and L. Green Jr., Academic Press, New York, 1964, pp. 485-522.

[5]Smoot, L.D. and Price, C.F., "Regression Rates of Nonmetalized Hybrid Fuel Systems," *AIAA Journal,* Vol. 3, Aug. 1965, pp. 1408-1413.

[6]Smoot, L.D. and Price, C.F., "Regression Rates of Metalized Hybrid Fuel Systems," *AIAA Journal,* Vol. 4, May 1966, pp. 910-915.

[7]Smoot, L.D. and Price, C.F., "Pressure Dependence of Hybrid Fuel Regression Rates," *AIAA Journal,* Vol. 5, Jan. 1967, pp. 102-106.

[8]Rastogi, R.P. and Baijal, S.K., "Heterogeneous Combustion of Boron-Containing Polymers," *AIAA Journal,* Vol. 9, Dec. 1971, pp. 2399-2403.

[9]Rastogi, R.P., Kishore, K., and Chaturvedi, B.K., "Heterogeneous Combustion Studies on Polystyrene and Styrene Copolymer," *AIAA Journal,* Vol. 12, Sept. 1974, pp. 1187-1192.

[10]Marxman, G.A., "Combustion in the Turbulent Boundary Layer on a Vaporizing Surface," *Proceedings of the Tenth Symposium (International) on Combustion,* The Combustion Institute, Pittsburgh, Pa., 1965, pp. 1337-1349.

[11]Marxman, G. and Gilbert, M., "Turbulent Boundary Layer Combustion in the Hybrid Rocket," *Proceedings of the Ninth Symposium (International) on Combustion,* Academic Press, N.Y., 1963, pp. 371-383.

[12]Wooldridge, C.E. and Muzzy, R.J., "Internal Ballistic Considerations in Hybrid Rocket Design," *Journal of Spacecraft,* Vol. 4, Feb. 1967, pp. 255-262.

[13]McAdams, H., *Heat Transmission,* McGraw-Hill, N.Y., 1954, p. 99.

[14]Godridge, A.M. and Hammond, E.G., "Emissivity of a Very Large Residual Oil Flame," *Proceedings of the Twelfth Symposium (International) on Combustion,* The Combustion Institute, Pittsburgh, Pa., 1969, pp. 1219-1228.

[15]Gaydon, A.G. and Wolfhard, H.G., *Flames: Their Structure, Radiation and Temperature,* Chapman and Hall Ltd., London, 1970, pp. 240-243.